

The Yeast Prion Protein Ure2 Shows Glutathione Peroxidase Activity in Both Native and Fibrillar Forms*

Received for publication, June 14, 2004, and in revised form, September 10, 2004
Published, JBC Papers in Press, September 15, 2004, DOI 10.1074/jbc.M406612200

Ming Bai^{‡§}, Jun-Mei Zhou^{‡¶}, and Sarah Perrett^{‡¶}

From the [‡]National Laboratory of Biomacromolecules, Institute of Biophysics, Chinese Academy of Sciences, 15 Datun Road, Chaoyang District, Beijing 100101, China and [§]Graduate School of the Chinese Academy of Sciences, 19 Yuquan Road, Fengtai District, Beijing 100039, China

Ure2p is the precursor protein of the *Saccharomyces cerevisiae* prion [URE3]. Ure2p shows homology to glutathione transferases but lacks typical glutathione transferase activity. A recent study found that deletion of the Ure2 gene causes increased sensitivity to heavy metal ions and oxidants, whereas prion strains show normal sensitivity. To demonstrate that protection against oxidant toxicity is an inherent property of native and prion Ure2p requires biochemical characterization of the purified protein. Here we use steady-state kinetic methods to characterize the multisubstrate peroxidase activity of Ure2p using GSH with cumene hydroperoxide, hydrogen peroxide, or *tert*-butyl hydroperoxide as substrates. Glutathione-dependent peroxidase activity was proportional to the Ure2p concentration and showed optima at pH 8 and 40 °C. Michaelis-Menten behavior with convergent straight lines in double reciprocal plots was observed. This excludes a ping-pong mechanism and implies either a rapid-equilibrium random or a steady-state ordered sequential mechanism for Ure2p, consistent with its classification as a glutathione transferase. The mutant 90Ure2, which lacks the unstructured N-terminal prion domain, showed kinetic parameters identical to wild type. Fibrillar aggregates showed the same level of activity as native protein. Demonstration of peroxidase activity for Ure2 represents important progress in elucidation of its role *in vivo*. Further, establishment of an *in vitro* activity assay provides a valuable tool for the study of structure-function relationships of the Ure2 protein as both a prion and an enzyme.

The glutathione *S*-transferases (GSTs)¹ are a multifunctional family of enzymes broadly distributed in nature that play a critical role in the cellular detoxification process (reviewed in Refs. 1–6). GSTs have the general function of conjugating GSH to electrophilic substances to reduce their toxicity. As a consequence, GSTs are involved in development of resistance toward drugs, insecticides, and herbicides and have a

protective role against a range of diseases including cancer. GSTs are dimeric proteins with a relatively conserved N-terminal thioredoxin-like domain and a more variable C-domain. GST activity is typically tested using the “universal” GST substrate, 1-chloro-2,4-dinitrobenzene (CDNB). However, a number of GSTs identified by structural criteria have failed to show activity toward CDNB (5). Some GSTs have been shown to have overlapping functions with other glutathione-binding enzymes such as glutathione peroxidases (GPxs) and glutaredoxins (1–3). These enzyme families share the GSH-binding thioredoxin domain but are otherwise structurally and mechanistically dissimilar (7–10). Characterization of the GSTs, glutaredoxins, and phospholipid hydroperoxide glutathione peroxidases present in *Saccharomyces cerevisiae* reveals some redundancy of function between the different classes of enzyme (11–13). The versatility of the glutathione-binding enzymes and their tendency to show overlapping functions may contribute significantly to the ability of the host organism to adapt to change.

Ure2p is the protein determinant of the *S. cerevisiae* prion [URE3] (14). Analogous to the mammalian prion (15), the heritable [URE3] prion phenotype is conveyed by a structural change in Ure2 to an aggregated form (16). It has recently been demonstrated that drugs isolated using a yeast prion cell-screening assay are also active against mammalian prions, suggesting that there may be features of the cellular mechanism of prion formation and/or maintenance that are common to yeast and mammalian prions despite the diversity of the proteins involved (17). Conversion of Ure2 to the prion form depends on the N-terminal ~90 amino acids (18). This N-terminal prion domain also directs the formation of amyloid-like fibrils *in vitro* (19, 20) and is predominantly unstructured in the native dimeric state (21, 22). Ure2 is involved in the regulation of nitrogen metabolism *in vivo*. This function is carried out by the C-terminal region of the protein and is lost on conversion to the prion form (16, 23). The crystal structure of the C-terminal region has been solved in both apo (24, 25) and glutathione-bound (26) forms, confirming the classification of Ure2 as a glutathione transferase (6, 23). However, attempts to demonstrate typical GST activity for Ure2, such as using CDNB, have so far proved unsuccessful (11, 21, 23, 27). A Ure2 homologue in *Aspergillus nidulans* was found to lack the nitrogen metabolite repression activity of Ure2 but contributed to heavy metal and xenobiotic resistance, including resistance to oxidative stress (28). Further, it was recently found that the deletion of the *S. cerevisiae* Ure2 gene increases the sensitivity of the cell to metals and cellular oxidants such as hydrogen peroxide (27, 29), raising the possibility that Ure2 possesses GPx activity. This has implications for the role of Ure2 *in vivo*. In addition, it implies the potential to establish an *in vitro* activity assay for Ure2, which would serve as an invaluable tool in structure-function analysis.

* This work was supported by the Natural Science Foundation of China (30070163, 30470363), the 973 Project of the Chinese Ministry of Science and Technology (G1999075608), and the Chinese Academy of Sciences Knowledge Innovation Project (KSCX2-SW214-3). The costs of publication of this article were defrayed in part by the payment of page charges. This article must therefore be hereby marked “advertisement” in accordance with 18 U.S.C. Section 1734 solely to indicate this fact.

[¶] Recipient of a special grant from the Chinese Academy of Sciences and research fellowships from the Royal Commission for the Exhibition of 1851 and the Royal Society. To whom correspondence may be addressed. Tel.: 86-10-64888496; Fax: 86-10-64840672; E-mail: sarah.perrett@iname.com or zhoujm@sun5.ibp.ac.cn.

¹ The abbreviations used are: GST, glutathione *S*-transferase; CDNB, 1-chloro-2,4-dinitrobenzene; GPx, glutathione peroxidase; CHP, cumene hydroperoxide; *t*-BH, *tert*-butyl hydroperoxide; ThT, thioflavin T.

In this study, we tested the activity of Ure2 toward a number of oxidant substrates *in vitro* to establish whether the peroxidase activity related to the Ure2 gene is an inherent property of the Ure2 protein. Having detected GPx activity for Ure2, we employed steady-state kinetic techniques to characterize the kinetic parameters for the substrates cumene hydroperoxide (CHP), *tert*-butyl hydroperoxide (*t*-BH), and H₂O₂ and to investigate the reaction mechanism. Further, we compared the activity of wild type Ure2 with that of a Ure2 deletion mutant, 90Ure2, which lacks the prion domain. Finally, we compared the activity of the native dimeric protein with that of fibrillar aggregates.

EXPERIMENTAL PROCEDURES

Materials—GSH, β -NADPH, CHP, *t*-BH, and glutathione reductase were from Sigma. Ure2 and 90Ure2 were produced in *Escherichia coli* with an N-terminal His₆ tag and purified by nickel affinity chromatography or produced without a tag and purified by a series of ionic exchange and gel filtration chromatographic steps, as described previously (21). Proteins were stored at -80°C in 50 mM Tris-HCl buffer, pH 8.4, containing 0.2 M NaCl and defrosted in a 25°C water bath immediately prior to use. The protein concentration in terms of monomers was measured by absorbance at 280 nm using an extinction coefficient of $40,700\text{ M}^{-1}\text{ cm}^{-1}$ (21) unless otherwise stated.

Enzyme Assays and Steady-state Kinetic Analysis—The GPx activity of Ure2 was determined using GSH with one of the hydroperoxides, CHP, H₂O₂, or *t*-BH, as substrates using a coupled spectrophotometric assay as described previously (30) with slight modifications. Unless otherwise indicated, the assay was carried out at 25°C in a 1-ml reaction volume containing 100 mM sodium phosphate buffer, pH 7.5, 4 mM sodium azide, 0.5–5.0 mM GSH, 0.15 mM β -NADPH, 0.24 units of glutathione reductase, and 0.3–3.0 μM Ure2. The reaction mixture was preincubated at 25°C for 6 min, after which the reaction was started by the addition of the hydroperoxide substrate to a final concentration of 0.5–5.0 mM to both cuvettes. The progress of reactions was monitored continuously by following the decrease in NADPH absorbance at 340 nm on a Shimadzu UV2501PC14 spectrophotometer. Initial rates were determined from the linear slope of progress curves obtained with an extinction coefficient for NADPH of $6220\text{ M}^{-1}\text{ cm}^{-1}$ after subtracting the non-enzymatic velocities due to the auto-oxidation of GSH by the hydroperoxide determined from the corresponding blank. When bovine serum albumin was used in place of Ure2, no increase over the base-line rate was observed. The presence or absence of 4 mM sodium azide had no effect on the Ure2 activity. When GSH was omitted from the reaction mixture, no Ure2 activity was observed.

Steady-state kinetic analysis was carried out by obtaining sets of initial velocities over a wide range of concentrations of one substrate while the concentration of the other substrate was kept constant (31, 32). The data were fitted to the Michaelis-Menten equation or the Lineweaver-Burk equation. The values obtained from these plots, and Eadie-Hofstee plots were the same within error. Single or global fitting was carried out using the regression wizard of SigmaPlot. The errors shown are the S.E. of the fit, or the mean \pm S.E. obtained from independent measurements, as appropriate.

Determination of true kinetic parameters and investigation of the reaction mechanism were performed by obtaining Michaelis-Menten curves at a series of concentrations of the second substrate and then fitting the data globally to the Michaelis-Menten model describing two-substrate sequential binding (32–34). The values obtained by linear extrapolation using secondary plots or by global fitting were the same within error.

Assay of Ure2 GPx Activity during the Time Course of Amyloid-like Fibril Formation—The initial sample was centrifuged at $18,000 \times g$ for 30 min at 4°C to remove any preexisting aggregates, and 300 μl of the supernatant was transferred into each of a series of tubes, one for each time point. The reaction mixture contained 30 μM full-length Ure2 in 50 mM sodium phosphate buffer, pH 7.5, containing 0.2 M NaCl. The samples were incubated in parallel at a constant temperature of 37°C with shaking as described previously (35, 36). Under these conditions, the increase in fluorescence due to ThT binding correlates directly with the appearance of fibrillar aggregates of Ure2 (36). At each time point, one of the samples was placed on ice. A 50- μl aliquot of the complete reaction mixture was removed and assayed for GPx activity using 1 mM GSH and 1.2 mM CHP as substrates, as described above. A further 10- μl aliquot of the reaction mixture was removed to assay for ThT binding, as described previously (35–37). After centrifugation of the remaining

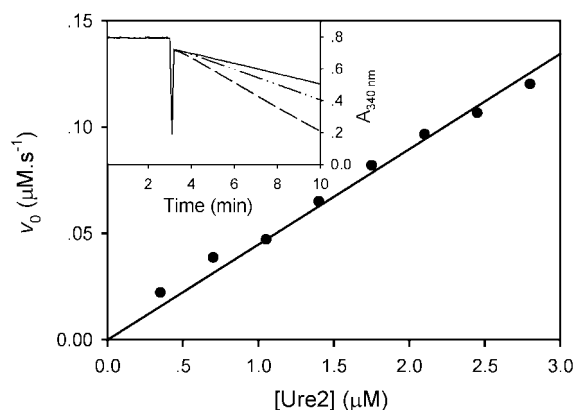


FIG. 1. **Glutathione-dependent reduction of CHP catalyzed by Ure2p.** The initial velocity of the Ure2-catalyzed reaction is plotted as a function of the Ure2 concentration. The reaction conditions were 100 mM sodium phosphate buffer, pH 7.5, 1 mM GSH, and 1.2 mM CHP at 25°C . Other details are as described under "Experimental Procedures." *Inset*, the non-enzymatic rate (solid line) was measured and subtracted from the reaction rate measured in the presence of Ure2 (1 μM (dashed-dotted line); 2.5 μM (dashed line)) in each case. In the absence of GSH, no reaction was observed.

240 μl of sample, a 50- μl aliquot of the resulting supernatant was assayed for GPx activity. A further 10- μl aliquot of supernatant was used for protein concentration determination using the method of Bradford (38). The precipitate was resuspended in 240 μl of the same buffer, and then a 50- μl aliquot of the resuspended mixture was assayed for GPx activity. Thus, the final protein concentration in the GPx assays was 1.5 μM for the total reaction mixture and a maximum of 1.5 μM in either the supernatant or the pellet fraction, depending on the relative distribution of protein between the fractions during the course of fibril formation. The pattern of change observed was highly reproducible in independent experiments.

RESULTS

Ure2 Shows Glutathione Peroxidase Activity—The ability of Ure2 to reduce hydroperoxides was tested *in vitro* using purified Ure2 with the oxidant substrate CHP and the reducing agent GSH. Reactions were followed by the oxidation of NADPH, which is coupled to the reduction of GSSG to GSH by glutathione reductase. The rate of non-enzymatic oxidation of NADPH in the absence of Ure2 was subtracted in each case. When Ure2 was added in the presence of all of the other components of the assay, a significant increase in the oxidation rate of NADPH was observed (Fig. 1, *inset*) and the initial velocity of the Ure2-catalyzed reaction was found to be proportional to the Ure2 concentration (Fig. 1, *main panel*). As is characteristic of an enzyme-catalyzed reaction (32), the enzymatic activity of Ure2 toward CHP showed pH and temperature optima, in this case at around pH 8.0 and 40°C (Fig. 2). In contrast, the uncatalyzed rate was observed to increase steeply above pH 8 or above 30°C (data not shown). Therefore, we adopted pH 7.5 and 25°C as the standard conditions for the Ure2 GPx activity assay. A control using bovine serum albumin in place of Ure2 over the same protein concentration range showed no detectable GPx activity (data not shown). The presence or absence of 4 mM sodium azide had no effect on the Ure2 GPx activity, ruling out the possibility that the observed activity is due to contamination with a heme-containing peroxidase such as catalase or myeloperoxidase. Ure2 showed no peroxidase activity in the absence of GSH. This then demonstrates that Ure2 has GSH-dependent peroxidase activity.

Comparison of Different Hydroperoxide Substrates—To further characterize the GPx activity of Ure2, we employed steady-state methods to obtain the apparent kinetic parameters for the enzymatic reaction. The results of steady-state kinetic analysis of Ure2 GPx activity toward the substrates

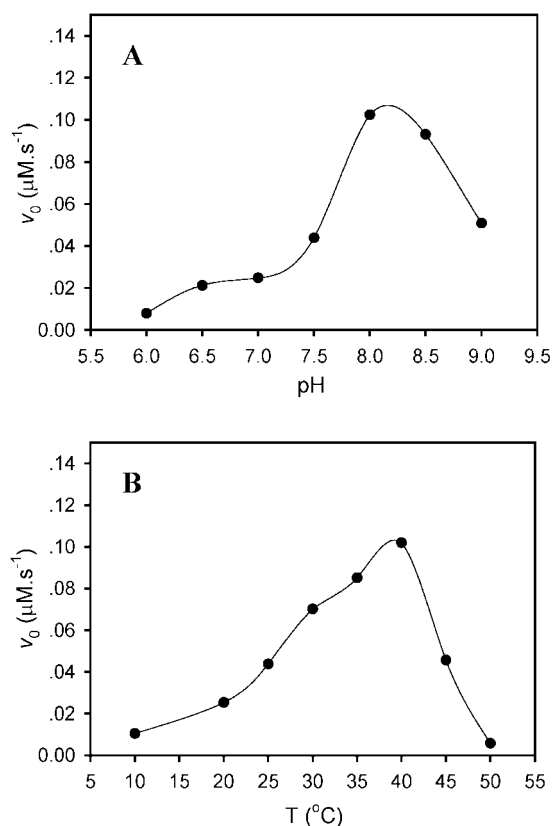


FIG. 2. Optima of Ure2 catalyzed glutathione peroxidase activity toward CHP. A, pH dependence of activity measured at 25 $^{\circ}\text{C}$. B, temperature dependence of activity measured at pH 7.5. The Ure2 concentration was 1.2 μM . Other details are as in Fig. 1.

CHP, hydrogen peroxide, and *t*-BH are shown in Fig. 3 and Table I. When the concentration of one substrate was fixed and the concentration of the other substrate was varied, the GPx activity was hyperbolic with respect to substrate concentration (Fig. 3) and double-reciprocal Lineweaver-Burk plots were linear (Fig. 4), as is typical of adherence to Michaelis-Menten kinetics (31). Ure2 showed activity toward all three substrates with an apparent preference in the order $\text{H}_2\text{O}_2 \geq \text{CHP} > t\text{-BH}$. This indicates that Ure2 has GPx activity toward hydrogen peroxide as well as typical organic hydroperoxide substrates.

The Prion Domain Does Not Contribute to Peroxidase Activity—The apparent kinetic parameters obtained for wild type Ure2 (with and without a His₆ tag) and for the prion domain deletion mutant 90Ure2 are shown in Table II. The results show that not only does the presence of a His₆ tag have no effect on the enzymatic activity of Ure2 but also that the detected activity cannot be attributed to contamination with a similar enzyme, given the radically different purification methods for tagged and non-tagged protein (see “Experimental Procedures”). The parameters obtained for 90Ure2 are the same within error as those obtained for wild type Ure2, indicating that the prion domain does not contribute to the GPx activity. This result is consistent with the finding that the Ure2 prion domain is essentially unstructured in the native dimer (21, 22) and has no effect on the stability or folding of Ure2 (21, 39).

Investigation of the Reaction Mechanism and Determination of True Kinetic Parameters—To further investigate the mechanism of Ure2 GPx activity, we obtained a data set of initial velocities over a wide range of GSH and CHP concentrations. The exact steady-state solutions of the mechanisms for two-substrate reactions are extremely complicated. However, in practice, only a limited number of mechanisms are observed

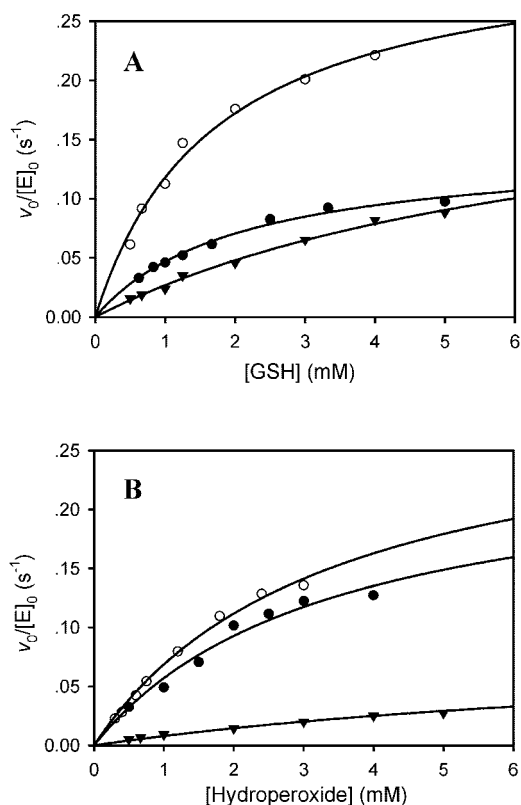


FIG. 3. GPx activity of Ure2p with different hydroperoxide substrates measured under steady-state conditions. The fit to the Michaelis-Menten equation is shown. The Ure2 concentration was 0.6–1.3 μM . A, varying concentrations of GSH with a fixed hydroperoxide substrate concentration of 1.2 mM for CHP (●) or H_2O_2 (○) and 5 mM for *t*-BH (▼). B, varying concentrations of hydroperoxide substrates with a fixed GSH concentration of 1 mM. Symbols are as in A.

and, under certain conditions, the rate equations can be reduced to simple forms (31–34). Fig. 4 shows double-reciprocal plots of the initial velocity *versus* one substrate concentration, obtained for a range of concentrations of the second substrate. The slope of the lines was observed to decrease with increasing concentration of the second substrate, and the lines intersected at a common point. This rules out a ping-pong mechanism (which is characterized by parallel double-reciprocal plots). The pattern observed is consistent with a sequential mechanism, and the data can be fitted to Equation 1 (32–34),

$$v = \frac{V_{\max}[A][B]}{K_{iA}K_{mB} + K_{mB}[A] + K_{mA}[B] + [A][B]} \quad (\text{Eq. 1})$$

where K_{mA} and K_{mB} are the Michaelis constants for substrates A and B, respectively, and K_{iA} is the inhibition constant for substrate A (which under certain circumstances is equal to the dissociation constant for A binding to the enzyme). It has been demonstrated there are two situations where the form of the equation simplifies in this way (32, 33), namely, a rapid-equilibrium random mechanism or a compulsorily ordered mechanism (Fig. 5). Because of the equivalent form of the rate equations, it cannot be distinguished from the current data whether binding is random or ordered. However, if binding is ordered, given that GSH binds to Ure2 in the absence of a second substrate (26), GSH must bind first. The true kinetic parameters obtained by fitting of the data shown in Fig. 4 to Equation 1 are shown in Table III.

Ure2 Fibrillar Aggregates Show Peroxidase Activity—Ure2 was incubated under conditions that have been thoroughly characterized by electron microscopy and atomic force microscopy and that promote rapid and abundant fibril formation (35,

TABLE I
Apparent steady-state kinetic constants for Ure2 activity toward different hydroperoxide substrates

The apparent kinetic constants were determined from Michaelis-Menten plots of initial velocities *versus* varying concentrations of one substrate with a fixed concentration of the other substrate under standard assay conditions as described under "Experimental Procedures" and shown in Fig. 3. The Ure2 concentration, $[E]_0$, was 0.6–1.3 μM . The values shown are the mean \pm S.E. of repeated measurements.

Substrate	Fixed [hydroperoxide substrate] ^a		Fixed [GSH] at 1 mM	
	$K_m(\text{GSH})_{(\text{app})}$ mM	$V_{\text{max}(\text{app})}/[E]_0$ s^{-1}	$K_m(\text{app})$ mM	$V_{\text{max}(\text{app})}/[E]_0$ s^{-1}
CHP	2.6 ± 0.1	0.12 ± 0.02	7.8 ± 0.2	0.37 ± 0.02
H ₂ O ₂	2.1 ± 0.4	0.36 ± 0.05	4.3 ± 0.9	0.36 ± 0.06
<i>t</i> -BH	5.5 ± 1.0	0.16 ± 0.04	7.9 ± 2.9	0.07 ± 0.02

^a Fixed [CHP] or [H₂O₂] at 1.2 mM; fixed [*t*-BH] at 5 mM.

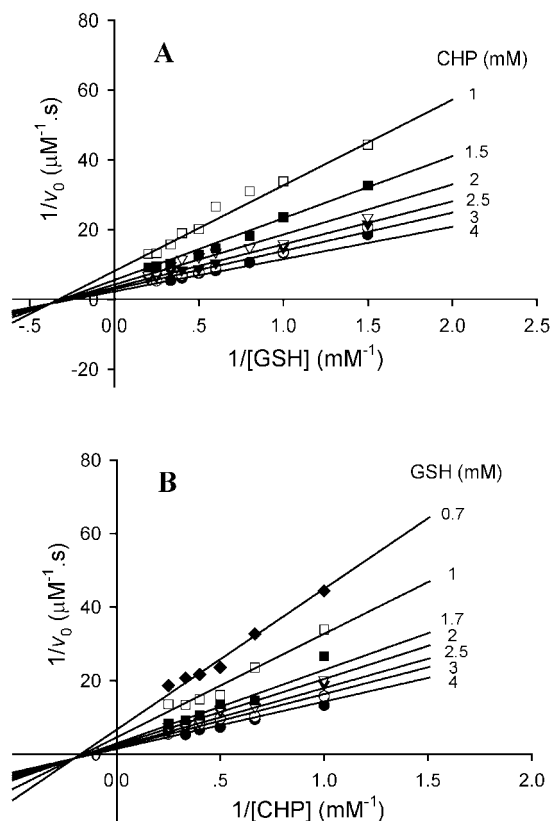


FIG. 4. Double-reciprocal plots of Ure2p activity at a fixed concentration of one substrate *versus* varying concentrations of the second substrate for GSH and CHP. The concentration of Ure2p in the reactions was 0.6 μM . The observed pattern of intersecting straight lines excludes a ping-pong reaction mechanism and is consistent with either a steady-state ordered sequential mechanism or a rapid-equilibrium random sequential mechanism. The parameters obtained by global fitting of the data to Equation 1 are shown in Table III.

36). Under these conditions, it was found that the increase in the binding fluorescence of the amyloid-specific dye ThT correlates directly with the time dependent appearance of fibrillar aggregates of Ure2, providing a convenient method to quantify the extent of fibril formation (36). Aliquots were removed at regular time intervals for analysis (see "Experimental Procedures"). The course of fibril formation was monitored by assaying the ThT binding of the incubation mixture and by measuring the decrease in the protein concentration in the supernatant fraction subsequent to sedimentation of the aggregates (Fig. 6A). In parallel, the GPx activity was assayed for the complete reaction mixture, and for the supernatant and pellet fractions (Fig. 6B). Concomitant with the formation of fibrillar aggregates and the loss of protein from the supernatant fraction, the GPx activity of the solution was lost from the supernatant fraction and instead was found in the pellet fraction. The level of activity of the complete incubation mixture, or of

the sum of the pellet and supernatant fractions, remained almost constant throughout the course of the experiment (Fig. 6B). This then indicates that Ure2 GPx activity is maintained within ordered aggregates and suggests that the level of activity is essentially unaffected by fibril formation, at least under the conditions used here.

DISCUSSION

The bovine spongiform encephalopathy epidemic (40) and the subsequent emergence of a new variant of the equivalent human disease (41) has prompted a massive worldwide effort to understand the prion phenomenon (15). The finding that prions also exist in fungi (14) has contributed significantly to establishing the viability of the prion concept (42). To understand the molecular mechanism of prion formation requires characterization of the structural and folding properties of the prion proteins. The natural tendency of prion proteins to aggregate makes this a difficult task. Nevertheless, significant progress has been made in recent years. High resolution structures are available for the mammalian prion protein, PrP (43, 44), and for Ure2 (24–26). In addition, the stability and kinetics of folding have been studied by a number of spectroscopic methods for PrP (45–47) and Ure2 (20, 21, 35, 39, 48, 49). The disadvantage of purely spectroscopic methods for folding studies is that it is often difficult to separate the native-structure signal from those of native-like or partially folded states. Therefore, the availability of an assay for native activity is an extremely important tool in structure-function analysis (31). In the case of Ure2, it was found that the native state could be distinguished from a spectroscopically identical misfolded native-like state by the difference in their unfolding kinetics (39). However, this unfolding assay requires the addition of high concentrations of chemical denaturant and is not readily applicable to fibrillar aggregates. Thus, the establishment of an *in vitro* activity assay for Ure2, as described here, not only addresses questions regarding the physiological structure and function of Ure2 but also provides an important tool for further mechanistic analysis of Ure2 as both an enzyme and a prion.

Ure2 showed glutathione-dependent peroxidase activity toward both hydrogen peroxide and standard organic hydroperoxide substrates (Fig. 3 and Table I). This finding indicates that Ure2, while lacking typical GST activity (23), nevertheless belongs to the subset of GST proteins that are active against oxidant substrates (1, 5). Most GPxs contain a selenocysteine, which reacts covalently with GSH, generally via a ping-pong enzyme reaction mechanism (7). In contrast, GSTs use a conserved tyrosine, serine, or cysteine residue to interact with the thiol group of GSH, thus increasing the reactivity of GSH, typically via a sequential mechanism (8–10). Thus, the observation of a sequential mechanism for Ure2 peroxidase activity (Figs. 4 and 5) is in agreement with the designation of Ure2 as a GST. The residue Asn¹²⁴ has been suggested as a candidate for the catalytically essential residue in the Ure2 GSH-binding domain (26), although this remains in question, particularly

TABLE II
Apparent steady-state kinetic constants for Ure2 and 90Ure2

Details are as for Table I.

Protein	Fixed [CHP] at 1.2 mM		Fixed [GSH] at 1 mM	
	$K_m(\text{GSH})_{\text{(app)}}$	$V_{\text{max(app)}/[E]_0}$	$K_m(\text{CHP})_{\text{(app)}}$	$V_{\text{max(app)}/[E]_0}$
	mM	s^{-1}	mM	s^{-1}
Ure2 (no tag)	2.6 ± 0.4	0.14 ± 0.02	7.1 ± 0.6	0.39 ± 0.04
Ure2	2.6 ± 0.1	0.12 ± 0.02	7.8 ± 0.2	0.37 ± 0.02
90Ure2	2.4 ± 0.1	0.14 ± 0.02	7.7 ± 0.5	0.42 ± 0.03

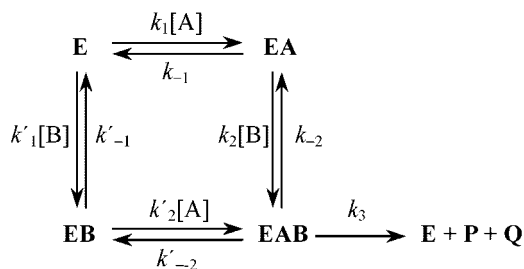


FIG. 5. **Minimal scheme for a sequential enzyme reaction mechanism.** The enzyme, E , binds to two substrates, A and B , to give products, P and Q . In a rapid-equilibrium situation, the binding of the substrates is rapid compared with the rate of the reaction. The reaction may be ordered with a particular substrate always binding first, or the sequence of substrate binding may be random.

TABLE III
True kinetic constants for Ure2 derived from steady-state kinetic analysis

The kinetic parameters were measured using the coupled enzyme assay with $[\text{Ure2}] = 0.6 \mu\text{M}$, $[\text{GSH}] = 0.7 - 4.0 \text{ mM}$, and $[\text{CHP}] = 1.0 - 4.0 \text{ mM}$ to obtain a series of sets of data as shown in Fig. 4. The parameters were obtained by global fitting of the data to Equation 1. The errors shown are the S.E. of the fit.

Kinetic parameter	Value	Method of determination
k_{cat}	$1.9 \pm 0.3 \text{ s}^{-1}$	$V_{\text{max}}/[E]_0$
$K_m(\text{GSH})$	$4.8 \pm 0.6 \text{ mM}$	Measured
$K_m(\text{CHP})$	$7.4 \pm 1.4 \text{ mM}$	Measured
$K_I(\text{GSH})$	$3.2 \pm 0.5 \text{ mM}$	Measured
$K_m(\text{CHP})$	$4.9 \pm 1.3 \text{ mM}$	$K_I(\text{GSH})K_m(\text{CHP})/K_m(\text{GSH})$
$k_{\text{cat}}/K_m(\text{GSH})$	$4.0 \pm 0.8 \times 10^2 \text{ M}^{-1} \text{ s}^{-1}$	$k_{\text{cat}}/K_m(\text{GSH})$
$k_{\text{cat}}/K_m(\text{CHP})$	$2.6 \pm 0.7 \times 10^2 \text{ M}^{-1} \text{ s}^{-1}$	$k_{\text{cat}}/K_m(\text{CHP})$

because enzymatic activity had not been demonstrated until now (25). The establishment of an assay for Ure2 activity paves the way for mutagenesis studies to define the residues required for Ure2 catalytic activity.

The kinetic parameters measured for Ure2, namely K_m values in the millimolar range and k_{cat}/K_m values in the 10^2 – 10^3 range (Table III), are consistent with the values observed for related enzymes. For example, the *S. cerevisiae* GSTs (which react with CDNB but not with hydroperoxides) also showed apparent $K_m(\text{GSH})$ values in the millimolar range (11). The *S. cerevisiae* glutaredoxins showed apparent k_{cat}/K_m values of around 10^3 for CDNB and 10^4 for CHP with apparent substrate K_m values in the millimolar range (12). The apparent specificity constant for the bacterial GST from *Proteus mirabilis* reacting with CDNB is around $10^3 \text{ M}^{-1} \text{ s}^{-1}$ with an apparent $K_m(\text{GSH})$ of 0.34 mM and an apparent $K_m(\text{CDNB})$ of 2.5 mM (10). The observation of oxidant sensitivity for Ure2 mutants (27), combined with demonstration here that peroxidase activity is an inherent property of the Ure2 protein, indicates that Ure2 is functional in *S. cerevisiae* cells as a peroxidase.

A particularly interesting and controversial aspect of the Ure2 prion protein is its ability to assemble into amyloid-like fibrils (19, 22, 36) while still retaining native-like structural properties (50, 51). We observed the same level of GPx activity in fibrillar aggregates of Ure2 as for the same concentration of

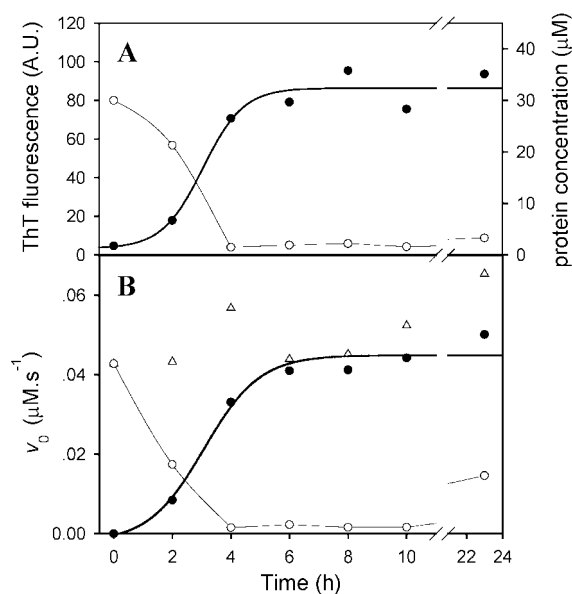


FIG. 6. **Relationship between peroxidase activity and the time course of fibril formation.** Incubation was in 50 mM sodium phosphate buffer, pH 7.5, 0.2 M NaCl at 37 °C with shaking, conditions that strongly favor fibril formation (35, 36). A, fibril formation was monitored by assaying changes in ThT binding (●) and by measuring the protein concentration in the supernatant fraction after centrifugation (○). B, in parallel, the GPx activity in the resuspended pellet fraction (●), supernatant fraction (○), and total reaction mixture (Δ) was assayed. The initial velocities are shown for a final protein concentration in the GPx assay of 1.5 μM for the total reaction mixture and a maximum of 1.5 μM in either the pellet or the supernatant fraction, depending on the distribution of the protein between the fractions over time.

fully dispersed soluble protein (Fig. 6). This finding is consistent with the observation that fibrillar aggregates of Ure2 maintain the ability to bind GSH (50) and fibrils formed from other enzymes linked to the Ure2 prion domain can still react with their specific substrates, provided that the substrate is small enough to diffuse into the fibrillar arrays (51). In principle, the kinetics of an immobilized enzyme may be different from the kinetics of the enzyme free in solution because of one or more of the following factors: 1) a change in conformation; 2) a change in environment; 3) a change in the effective concentration of the substrate; or 4) diffusional effects (52). Diffusional effects will be negligible if the substrate can easily reach the enzyme, or if catalysis is slow with respect to diffusion (*i.e.* k_{cat}/K_m is low) as is the case for Ure2. The results presented here provide direct support for the suggestion that formation of fibrillar aggregates of Ure2 does not involve significant structural change within the C-terminal globular region but rather that the native-like structure and activity are preserved. This finding then supports the hypothesis that a loss of nitrogen metabolite repression in the [URE3] prion state is due to a steric blocking mechanism, rather than to a loss of native-like Ure2 structure (51). Furthermore, these results are consistent with the observation that prion strains show normal sensitivity to oxidant stress (27), indicating that the Ure2 fibril formation assay is an

excellent model for the structural changes accompanied by prion formation in yeast cells. The availability of a convenient and relevant *in vitro* assay system to conduct structure-function analysis will allow further investigation of the interplay of the various roles of Ure2: as a regulator of nitrogen metabolism, a detoxification enzyme, and a prion.

Acknowledgments—We thank Prof. Z. X. Wang, Prof. X. M. Pan, and Dr. H. Wu of this institute and Dr. L. Itzhaki (University of Cambridge) for advice and helpful discussions.

REFERENCES

- Sheehan, D., Meade, G., Foley, V. M., and Dowd, C. A. (2001) *Biochem. J.* **360**, 1–16
- Armstrong, R. N. (1997) *Chem. Res. Toxicol.* **10**, 2–18
- Mannervik, B., Cameron, A. D., Fernandez, E., Gustafsson, A., Hansson, L. O., Jemth, P., Jiang F., Alwyn Jones, T., Larsson, A. K., Nilsson, L. O., Olin, B., Pettersson, P. L., Ridderström, M., Stenberg, G., and Widersten, M. (1998) *Chem. Biol. Interact.* **111–112**, 15–21
- Board, P. G., Cogga, M., Chelvanayagam, G., Eastale, S., Jermiin, L. S., Schulte, G. K., Danley, D. E., Hoth, L. R., Griffor, M. C., Kamath, A. V., Rosner, M. H., Chrunyk, B. A., Perregaux, D. E., Gabel, C. A., Geoghegan, K. F., and Pandit, J. (2000) *J. Biol. Chem.* **275**, 24798–24806
- Vuilleumier, S. (1997) *J. Bacteriol.* **179**, 1431–1441
- Rosjohn, J., Board, P. G., Parker, M. W., and Wilce, M. C. J. (1996) *Protein Eng.* **9**, 327–332
- Saito, Y., Hayashi, T., Tanaka, A., Watanabe, Y., Suzuki, M., Saito, E., and Takahashi, K. (1999) *J. Biol. Chem.* **274**, 2866–2871
- Nay, B., Fournier, D., Baudras, A., and Baudras, B. (1999) *Insect Biochem. Mol. Biol.* **29**, 71–79
- Labrou, N. E., Mello, L. V., and Clonis, Y. D. (2001) *Biochem. J.* **358**, 101–110
- Caccuri, A. M., Antonini, G., Allocati, N., Di Ilio, C., De Maria, F., Innocenti, F., Parker, M. W., Masulli, M., Lo Bello, M., Turella, P., Federici, G., and Ricci, G. (2002) *J. Biol. Chem.* **277**, 18777–18784
- Choi, J. H., Lou, W., and Vancura, A. (1998) *J. Biol. Chem.* **273**, 29915–29922
- Collinson, E. J., and Grant, C. M. (2003) *J. Biol. Chem.* **278**, 22492–22497
- Avery, A. M., and Avery, S. V. (2001) *J. Biol. Chem.* **276**, 33730–33735
- Wickner, R. B. (1994) *Science* **264**, 566–569
- Prusiner, S. B. (1998) *Proc. Natl. Acad. Sci. U. S. A.* **95**, 13363–13383
- Masison, D. C., and Wickner, R. B. (1995) *Science* **270**, 93–95
- Bach, S., Talarek, N., Andrieu, T., Vierfond, J. M., Mettey, Y., Galo, H., Dormont, D., Meijer, L., Cullin, C., and Blondel, M. (2003) *Nat. Biotechnol.* **21**, 1075–1081
- Masison, D. C., Maddelein, M. L., and Wickner, R. B. (1997) *Proc. Natl. Acad. Sci. U. S. A.* **94**, 12503–12508
- Taylor, K. L., Cheng, N., Williams, R. W., Steven, A. C., and Wickner, R. B. (1999) *Science* **283**, 1339–1342
- Thual, C., Bousset, L., Komar, A. A., Walter, S., Buchner, J., Cullin, C., and Melki, R. (2001) *Biochemistry* **40**, 1764–1773
- Perrett, S., Freeman, S. J., Butler, P. J. G., and Fersht, A. R. (1999) *J. Mol. Biol.* **290**, 331–345
- Thual, C., Komar, A. A., Bousset, L., Fernandez-Bellot, E., Cullin, C., and Melki, R. (1999) *J. Biol. Chem.* **274**, 13666–13674
- Coshigano, P. W., and Magasanik, B. (1991) *Mol. Cell. Biol.* **11**, 822–832
- Bousset, L., Berlhali, H., Janin, J., Melki, R., and Morera, S. (2001) *Structure* **9**, 39–46
- Umlaud, T. C., Taylor, K. L., Rhee, S., Wickner, R. B., and Davis, D. R. (2001) *Proc. Natl. Acad. Sci. U. S. A.* **98**, 1459–1464
- Bousset, L., Berlhali, H., Melki, R., and Morera, S. (2001) *Biochemistry* **40**, 13564–13573
- Rai, R., Tate, J. J., and Cooper, T. G. (2003) *J. Biol. Chem.* **278**, 12826–12833
- Fraser, J. A., Davis, M. A., and Hynes, M. J. (2002) *Appl. Environ. Microbiol.* **68**, 2802–2808
- Basu, U., Southron, J. L., Stephens, J. L., and Taylor, G. J. (2004) *Mol. Gen. Genomics* **271**, 627–637
- Flohe, L., and Gunzler, W. A. (1984) *Methods Enzymol.* **104**, 115–121
- Fersht, A. R. (1998) *Structure and Mechanism in Protein Science*, W. H. Freeman, San Francisco
- Laidler, K. J., and Bunting, P. S. (1973) *The Chemical Kinetics of Enzyme Action*, Oxford University Press, Oxford
- Seubert, P. A., Renosto, F., Knudson, P., and Segel, I. H. (1985) *Arch. Biochem. Biophys.* **240**, 509–523
- Wu, H., Zheng, Y., and Wang, Z. X. (2003) *Biochemistry* **42**, 1129–1139
- Zhu, L., Zhang, X. J., Wang, L. Y., Zhou, J. M., and Perrett, S. (2003) *J. Mol. Biol.* **328**, 235–254
- Jiang, Y., Li, H., Zhu, L., Zhou, J. M., and Perrett, S. (2004) *J. Biol. Chem.* **279**, 3361–3369
- Uversky, V. N., Li, J., and Fink, A. L. (2001) *J. Biol. Chem.* **276**, 44284–44296
- Bradford, M. M. (1976) *Anal. Biochem.* **72**, 248–254
- Galani, D., Fersht, A. R., and Perrett, S. (2002) *J. Mol. Biol.* **315**, 213–227
- Hope, J., Reekie, L. J., Hunter, N., Multhaup, G., Beyreuther, K., White, H., Scott, A. C., Stack, M. J., Dawson, M., and Wells, G. A. (1988) *Nature* **336**, 390–392
- Will, R. G., Ironside, J. W., Zeidler, M., Cousens, S. N., Estibeiro, K., Alperovitch, A., Poser, S., Pocchiari, M., Hofman, A., and Smith, P. G. (1996) *Lancet* **347**, 921–925
- Tuite, M. F., and Cox, B. S. (2003) *Nature Rev. Mol. Cell. Biol.* **4**, 878–888
- Riek, R., Hornemann, S., Wider, G., Billeter, M., Glockshuber, R., and Wuthrich, K. (1996) *Nature* **382**, 180–182
- Zahn R., Liu, A., Luhrs, T., Riek, R., von Schroetter, C., Lopez Garcia, F., Billeter, M., Calzolari, L., Wider, G., and Wuthrich, K. (2000) *Proc. Natl. Acad. Sci. U. S. A.* **97**, 145–150
- Torrent, J., Alvarez-Martinez, M. T., Heitz, F., Liautard, J. P., Balny, C., and Lange, R. (2003) *Biochemistry* **42**, 1318–1325
- Apetri, A. C., Surewicz, K., and Surewicz, W. K. (2004) *J. Biol. Chem.* **279**, 18008–18014
- Hosszu, L. L., Jackson, G. S., Trevitt, C. R., Jones, S., Batchelor, M., Bhelt, D., Prodromidou, K., Clarke, A. R., Waltho, J. P., and Collinge, J. (2004) *J. Biol. Chem.* **279**, 28515–28521
- Zhou, J. M., Zhu, L., Balny, C., and Perrett, S. (2001) *Biochem. Biophys. Res. Commun.* **287**, 147–152
- Zhu L., Kihara, H., Kojima, M., Zhou, J. M., and Perrett, S. (2003) *Biochem. Biophys. Res. Commun.* **311**, 525–532
- Bousset, L., Thomson, N. H., Radford, S. E., and Meiki, R. (2002) *EMBO J.* **21**, 2903–2911
- Baxa, U., Speransky, V., Steven, A. C., and Wickner, R. B. (2002) *Proc. Natl. Acad. Sci. U. S. A.* **99**, 5253–5260
- Laidler, K. J., and Bunting, P. S. (1980) *Methods Enzymol.* **64**, 227–248